2011 American Control Conference
on O'Farrell Street, San Francisco, CA, USA
June 29 - July 01, 2011

# Capacity Estimation for Li-ion Batteries

Xidong Tang, Xiaofeng Mao, Jian Lin, and Brian Koch

*Abstract*—**This paper presents onboard capacity estimation algorithms for Li-ion batteries deployed in plug-in hybrid electric vehicles (PHEV) and electric vehicles (EV). Capacity estimation algorithms are developed based on an equivalent circuit model. The onboard estimation of battery capacity is treated separately for the driving mode and plug-in charge mode. Evaluation results on laboratory collected data and vehicle data show the effectiveness of the developed algorithms.**

## I. Introduction

Plug-in hybrid electric vehicles (PHEV) and electric vehicles (EV) are of great interest in today's automotive industry due to the urgent need for improved fuel economy and reduced emission. An efficient and reliable battery system is the key to the commercial success of PHEV and EV. Li-ion batteries provide higher power and energy densities than other existing batteries such as Ni-Mh and Ni-Cd systems [1-5], and become promising in the PHEV/EV applications.

To achieve an optimized performance and a long operating life of a battery, the knowledge of battery state of health (SOH) is necessary in addition to the knowledge of battery state of charge (SOC). While control strategies are designed based on battery SOC for short term targets, they need to be adjusted based on battery SOH for long term objectives. There are two main aspects defining a battery's SOH, that is, power capability and energy capability. For PHEV and EV applications, the energy capability, which determines the achievable electric range (the range achieved on electrical power solely) for a vehicle, is defined by the battery capacity. The battery capacity reflects how much energy in terms of Ampere-Hours can be stored into a fully charged battery, and thus is widely used as an indicator of battery SOH. As a battery ages, its capacity decreases, resulting in less energy. Given a specific driving profile, the loss of battery capacity leads to a reduced electric range for PHEV/EV. Numerous studies have shown the gradual fade of capacity over time for Li-ion batteries under extended cycling. However it is still an open topic to accurately estimate battery capacity in vehicles.

Li-ion battery dynamic behavior is a result of a complex electrochemical process, which has proven difficult to establish a practical battery model for vehicle implementation even after model simplification. Insufficient knowledge about Li-ion battery aging processes also challenges the design of accurate and robust battery capacity estimation algorithms. Traditionally the battery capacity can only be measured offline by depleting a fully charged battery with a certain current rate at a specific temperature. Obviously this method is impractical for in-vehicle applications. Furthermore since a full charge and discharge cycle can cause irreparable damage to the battery, the method is highly undesirable.

There exist a number of approaches for battery capacity estimation in the literature. Most of the existing approaches [1-3] are either inaccurate or impractical for in-vehicle applications. Other methods [4-5] are based on the so-called battery life models, which are predetermined usage models, and have limited adaptability in the real life environment. Another type of battery model is based on the electrochemical and thermodynamics principles [6], where the finite element analysis method is applied to solve a set of PDEs that are established to describe the Li-ion battery dynamics. The model is very useful to help understand the battery dynamic behavior. However, it is difficult to use the model for battery capacity estimation directly.

The electrical property of Li-ion batteries can be modeled as electrical circuits [7-9]. Typically, the open-circuit voltage is modeled as a capacitor or a voltage source. A resistor models the battery's internal resistance. Additional circuit components, such as RC pairs, can be used to model the battery's different dynamics. These types of models can be as complex or as simple as needed. The values of these electrical components such as resistors and capacitors are subject to temperature, SOC, and SOH. Capacity fade can be reflected through the change of some of the component values.

This paper discusses several practical solutions to onboard battery capacity estimation based on an equivalent circuit model. Algorithms are developed separately for two different operation modes: the driving mode and plug-in charge mode. The algorithms are evaluated through laboratory collected aging data and vehicle data, showing good estimation results.

## II. Battery Circuit Model

As equivalent circuits are widely used to model different types of batteries as in [7-9], this paper uses this technique to characterize the electrical property of Li-ion batteries. In this paper, a second-order equivalent circuit model is adopted to describe the dynamics of Li-ion batteries. The order of the model is determined through a standard hybrid pulse power characterization (HPPC) test. Readers can refer to [12] for the details of model identification.

The diagram of the second-order equivalent circuit model

Manuscript received September 27, 2010.

Xidong Tang is with General Motors, Global R&D, 30500 Mound Road, Warren, MI 48090 USA (phone: 586-298-0254; fax: 586-986-3003; e-mail: xidong.tang@gm.com).

Xiaofeng Mao is with General Motors, Global R&D, 30500 Mound Road, Warren, MI 48090 USA (e-mail: xiaofeng.mao@gm.com).

Jian Lin is with General Motors, Global Vehicle Engineering, 30001 Van Dyke Road, Warren, MI 48090 USA (e-mail: jian.lin@gm.com).

Brian Koch is with General Motors, Global Vehicle Engineering, 30001 Van Dyke Road, Warren, MI 48090 USA (e-mail: brian.j.koch@gm.com).

with two RC pairs is shown in Fig. 1. The two-RC-pair equivalent circuit model captures two main chemical processes: the diffusion and double layer. In Fig. 1, $R_{ct}$ is the charge transfer resistance, $C_{dl}$ is the double layer capacitance, $R_{df}$ is the diffusion resistance, and $C_{df}$ is the diffusion capacitance. The $R_{ct}$-$C_{dl}$ pair is used to account for the dynamics of the double layer, and the $R_{df}$-$C_{df}$ pair for the diffusion. In Fig. 1, $V_{oc}$ is the open circuit voltage (OCV), and $R_{ohm}$ is the ohmic resistance. The $V_{oc}$ is divided into two parts: $V_o$ and $V_h$, where $V_o$ is the thermodynamic voltage which has a one-to-one relationship to SOC, and $V_h$ represents the battery hysteresis voltage. The equivalent circuit model can represent both manganese-based Li-ion batteries and iron phosphate Li-ion batteries [12], while the hysteresis effect of manganese-based Li-ion batteries is negligible. In this paper, the discussion will be focused on manganese-based Li-ion batteries. Therefore, it is noted that $V_{oc} = V_o$ as $V_h = 0$ for manganese-based Li-ion batteries.

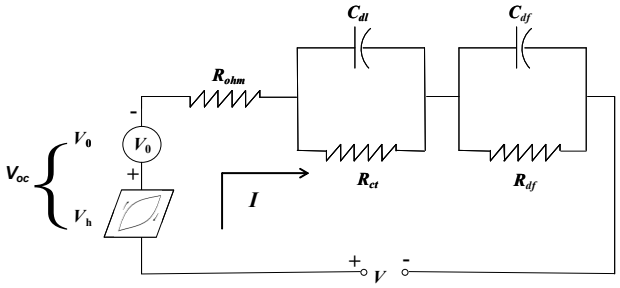


Fig. 1. The two-RC-pair battery circuit model for a Li-ion battery.

Battery capacity is defined as the stored charge in a fully charged battery, and SOC defines the remaining charge as a percentage of the capacity. With less capacity, the battery tends to store less charge in terms of Ampere-Hours (AH) at the same SOC level. It is also known that SOC is a monotonic function of OCV, i.e. a higher OCV indicating a higher SOC level. In other words, given the same OCV, an old battery with less capacity has less remaining charge than a new battery with more capacity. This observation is consistent with the well-known fact that the terminal voltage of a battery with less capacity tends to increase faster with the same amount of charge. It is further implied that capacity correlates with the change of OCV against current integration, i.e., $\Delta V_{oc}/\Delta S$, where $\Delta S = \int_{t=t_0}^{t=t_f} I(t)dt$ represents the current integration or charge accumulation over a certain time period $[t_0, t_f]$. This fact will be used as the basis for the development of capacity estimation algorithms in this paper.

It is also noticed that battery capacity is temperature dependent, as shown in Fig. 2. The estimated capacity reflects the actual capacity under the present temperature. In order to be used as a temperature-independent SOH index, the capacity estimated in real time needs to be normalized to a pre-defined temperature (e.g. 25ºC). The normalization can be done through a lookup table that maps the actual capacity to the normalized capacity in terms of temperatures. Such a lookup table can be established via experiments.

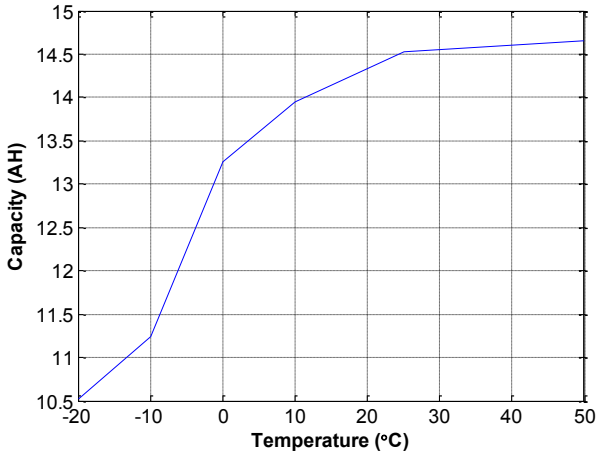


Fig. 2. Measured capacity at different temperatures for a Li-ion battery.

As illustrated by Fig. 1, the battery terminal voltage consists of four parts, which can be expressed as

$$V(k) = V_{oc}(k) + I(k)R_{ohm} + V_{dl}(k) + V_{df}(k) \qquad (1)$$

where $V_{oc}$ is the OCV, $R_{ohm}$ is the ohmic resistance, and $V_{dl}$ and $V_{df}$ (voltages across the two RC pairs) are the double layer voltage and the diffusion voltage, respectively. It should be noted that the change of $V_{oc}$, i.e. $\Delta V_{oc}$, is essential to capacity estimation. Therefore, in (1) $V_{oc}$ is not modeled as a constant parameter anymore, but a time varying signal.

As the battery capacity correlates with the change of OCV against current integration, we introduce a new parameter $h = \Delta V_{oc}/\Delta S$, which represents the change rate of OCV under a certain amount of current integration. From the discussion above, it is concluded that $h$ is related to the battery capacity and can be used to infer the battery capacity.

## III. Estimation In The Driving Mode

In the driving mode, the current varies as the power requirement from the electric propulsion changes. The current can be modeled as the input of the battery dynamic system. The voltage follows the current and is the output of the system. The frequent power transfer to/from batteries offers rich signal excitation to estimate the model parameters. Based on the two-RC-pair equivalent circuit model, two algorithms are developed to estimate capacity for the driving mode.

### *A. One Stage Estimation*

Following the discussion in [12], we have equations in the state space form to model the two-RC-pair equivalent circuit model in the discrete time domain, given by

$$\begin{bmatrix} V_{dl}(k) \\ V_{df}(k) \end{bmatrix} = A \begin{bmatrix} V_{dl}(k-1) \\ V_{df}(k-1) \end{bmatrix} + BI(k-1)$$
$$V(k) - V_{oc}(k) = C \begin{bmatrix} V_{dl}(k) \\ V_{df}(k) \end{bmatrix} + DI(k) \qquad (2)$$

where $A = \mathrm{diag}(a_1,\ a_2)$, $B = [b_1 \quad b_2]^T$, $C = [1 \quad 1]$, and $D = R$, and

$$\begin{aligned} a_1 &= \exp(-\Delta t/(R_{ct}C_{dl})) \\ b_1 &= R_{ct}\left(1-\exp(-\Delta t/(R_{ct}C_{dl}))\right) \\ a_2 &= \exp\left(-\Delta t/(R_{df}C_{df})\right) \\ b_2 &= R_{df}\left(1-\exp\left(-\Delta t/(R_{df}C_{df})\right)\right) \end{aligned} \tag{3}$$

and $\Delta t$ is the sampling time. The difference between (2) and the equations described in [12] is that in (2) $V_{oc}$ is not a constant, but a signal. This is because in order to capture the change of OCV for capacity estimation, the OCV cannot be modeled as a constant anymore.

The transfer function from the battery terminal current to the battery terminal voltage can be expressed as

$$\begin{aligned} V(z) - V_{oc}(z) &= C(zI_{2\times 2} - A)^{-1}BI(z) + DI(z) \\ &= \left(\frac{b_1(z-a_2)+b_2(z-a_1)}{(z-a_1)(z-a_2)} + R\right)I(z) \end{aligned} \tag{4}$$

By taking the inverse $z$-transform, the discrete-time model can be organized into the following difference equation:

$$\begin{aligned} V(k) = {} & (a_1+a_2)V(k-1) - a_1a_2V(k-2) + RI(k) \\ & +[b_1 - b_2 - (a_1+a_2)R]I(k-1) \\ & +(a_1a_1R - b_1a_2 - b_2a_1)I(k-2) + V_{oc}(k) \\ & -(a_1+a_2)V_{oc}(k-1) + a_1a_2V_{oc}(k-2). \end{aligned} \tag{5}$$

According to the definition of capacity and SOC, we have the following equation:

$$Q = \Delta S/\Delta\mathrm{SOC} \tag{6}$$

where $Q$ denotes the battery capacity, $\Delta S$ is the current integration or charge accumulation, and $\Delta$SOC denotes the change in SOC cause by $\Delta S$. With the new parameter $h = \Delta V_{oc}/\Delta S$ introduced in Section II, we rewrite (6) into

$$Q = \Delta S/\Delta\mathrm{SOC} = \Delta V_{oc}/(\Delta\mathrm{SOC} * h). \tag{7}$$

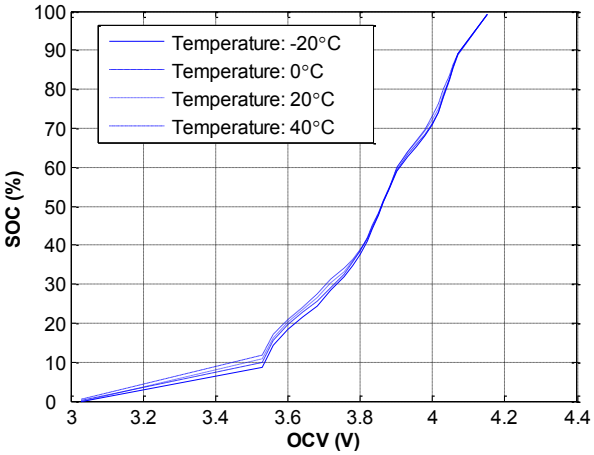

Fig. 3. SOC versus OCV curves at different temperatures.

It can be seen from (7) that the capacity $Q$ is inversely proportional to $h$ and can be calculated from $h$, if $\Delta V_{oc}/\Delta$SOC is known. In theory $\Delta V_{oc}/\Delta$SOC defines the slope of the OCV versus SOC curve, which can be obtained from experiments, as shown in Fig. 3. A lookup table covering the values of $\Delta V_{oc}/\Delta$SOC at various SOC and temperatures can thus be established. Now the problem of capacity estimation becomes to estimate the parameter $h$. Once $h$ is known, the capacity can be calculated using (7) and the lookup table.

As $h$ correlates with the change of OCV, the difference equation (5) is written in the form of the voltage increment: $\Delta V(k) = V(k) - V(k-1)$. From (5), it follows that

$$\begin{aligned} \Delta V(k) = {} & (a_1+a_2)\Delta V(k-1) - a_1a_2\Delta V(k-2) + R\Delta I(k) \\ & +[b_1+b_2-(a_1+a_2)R]\Delta I(k-1) \\ & +(a_1a_2R - a_2b_1 - a_1b_2)\Delta I(k-2) + \Delta V_{oc}(k) \\ & -(a_1+a_2)\Delta V_{oc}(k-1) + a_1a_2\Delta V_{oc}(k-2) \end{aligned} \tag{8}$$

where $\Delta V_{oc}(k) = V_{oc}(k) - V_{oc}(k-1)$. Note that

$$h = \Delta V_{oc}(k)/\Delta S(k) = \Delta V_{oc}(k)/(I(k-1)\,\Delta t) \tag{9}$$

Substituting (9) into (8), we rewrite (8) as

$$\begin{aligned} \Delta V(k) = {} & [1-(a_1+a_2)+a_1a_2]hI(k-1)\Delta t \\ & +(a_1+a_2)\Delta V(k-1) - a_1a_2\Delta V(k-2) + R\Delta I(k) \\ & +[b_1+b_2-(a_1+a_2)\mathrm{R} + (a_1+a_2-a_1a_2)h\Delta t]\Delta I(k-1) \\ & +(a_1a_2R - a_2b_1 - a_1b_2 - a_1a_2h\Delta t)\Delta I(k-2) \end{aligned} \tag{10}$$

which can be written into the following compact form:

$$\Delta V(k) = \theta^T\phi(k). \tag{11}$$

In (10), $\phi(k)$ is a vector of known signals defined as

$$\begin{aligned} \phi(k) = {} & [I(k-1)\Delta t, \Delta V(k-1), \Delta V(k-2) \\ & \Delta I(k), \Delta I(k-1), \Delta I(k-2)]^T, \end{aligned} \tag{12}$$

where $\Delta I(k) = I(k) - I(k-1)$, and $\theta = [\theta_1, \theta_2, \ldots, \theta_6]^T$ is a vector of unknown parameters. From (10), the elements of $\theta$ can be derived as follows:

$$\begin{aligned} \theta_1 &= [1-(a_1+a_2)+a_1a_2]h \\ \theta_2 &= a_1+a_2 \\ \theta_3 &= -a_1a_2 \\ \theta_4 &= R \\ \theta_5 &= b_1+b_2-a_1\mathrm{R}-a_2\mathrm{R}+(a_1+a_2-a_1a_2)h\Delta t \\ \theta_6 &= a_1a_2R - a_2b_1 - a_1b_2 - a_1a_2h\Delta t. \end{aligned} \tag{13}$$

The parameters in $\theta$ change with SOC and temperature, but can be assumed constant in a small region of SOC and temperature. From (13), it follows that $h$ can be inferred as

$$h = \theta_1/(1-\theta_2-\theta_3) \tag{14}$$

The task now becomes to estimate $\theta$ from the measured terminal voltage and terminal current. The estimated $\theta$ is then

used to calculate $h$ and in turn correlate with battery capacity. Many recursive estimation algorithms can be applied to estimate $\theta$. In this paper, the U-D factorization-based RLS estimation method [10-11] is used to estimate the battery parameters in (11). In the U-D factorization-based method, the positive definite covariance matrix $P$ is factorized as $P = UDU^T$, where $U$ is an upper triangular matrix and $D$ is a diagonal matrix. The matrix $P$ is not updated directly, instead, it is updated through multiplication of the updated values of $U$ and $D$. The U-D factorization-based RLS method has been successfully used in many industrial applications due to its computational efficiency and stability. Assuring the positive-definiteness and symmetry of the covariance matrix, the method can achieve high estimation accuracy and robustness. To compensate for shifting of $\theta$ due to the change of the operation condition, a forgetting factor is introduced.

Given a sequence of current $I(k)$ and voltage $V(k)$, the one stage estimation algorithm includes the following steps:

Step 1: The algorithm starts with initialization. Read $V(k)$ and $I(k)$, $k$=1,2. Set initials for $\theta$ as the estimate of last operation from nonvolatile memory (NVM). Set appropriate $U$ and $D$ for the initial covariance matrix. Set a forgetting factor $0 < \lambda \leq 1$.

Step 2: Read a new pair of data *V(k)* and *I(k)*.

Step 3: Update $\phi(k)$ using the present data $V(k)$ and $I(k)$, and the previous $V(k\text{-}1)$, $V(k\text{-}2)$, $I(k\text{-}1)$ and $I(k\text{-}2)$.

Step 4: Let $\alpha_0 = \lambda$. Define two vectors $f$ and $g$ as

$$f = [f_1, \dots, f_n]^T = U^T(k-1)\phi((k)$$
$$g = [g_1, \dots, g_n]^T = D(k-1)f. \quad (15)$$

Step 5: For $j = 1,2, \dots,6$, go through Step 5.1-5.2.

Step 5.1: Compute the following:

$$\alpha_j = \alpha_{j-1} + f_j g_j$$
$$D(k)_{jj} = (\alpha_{j-1} D(k-1)_{jj})/(\alpha_j \lambda)$$
$$b_j = g_j$$
$$c_j = -f_j/\alpha_{j-1}. \quad (16)$$

Step 5.2: For $i = 1,2, \dots, j-1$, go to Step 5.2.1 (if $j = 1$, skip Step 5.2.1).

Step 5.2.1: Compute the following:

$$U(k)_{ij} = U(k-1)_{ij} + b_i c_j$$
$$b_i = b_i + U(k-1)_{ij} b_j. \quad (17)$$

Step 6: Compute $L(k) = [b_1, \dots, b_n]^T/\alpha_n$.

Step 7: Compute the estimation error as

$$\beta(k) = \Delta V(k) - \theta^T(k-1)\phi((k). \quad (18)$$

Step 8: Update $\theta$ to minimize the estimation error $\beta$ by

$$\theta(k) = \theta(k-1) + L(k)\beta(k). \quad (19)$$

Step 9: Calculate the parameter $h$ from (14).

Step 10: Infer the capacity $Q$ from the table of $\Delta V_{oc}/\Delta\text{SOC}$.

Step 11: Determine the validity of the capacity estimate. If it is valid, normalize $Q$ in terms of temperature.

Step 12: If it is the end of operation, save $\theta$ to NVM for next operation. Otherwise, save $V(k)$ and $I(k)$ for next update. Go to Step 2 and continue the update.

### *B. Two Stage Estimation*

A two stage capacity estimation algorithm is developed for the driving mode too. In the first stage, the OCV is estimated from terminal voltage and current. Readers can refer to [12] for the details of onboard estimation of OCV. From the definition of capacity given by (6), the capacity can be calculated from $\Delta S$ and $\Delta\text{SOC}$. As suggested in the literature, the OCV monotonically increases with SOC. Therefore in the second stage, we use the OCV estimated from the first stage to get SOC information through an SOC-versus-OCV lookup table. Then the battery capacity is calculated as below:

$$Q(k) = \frac{\sum_{i=1}^{k-1} I(i)\Delta t}{\text{SOC}\,(k) - \text{SOC}\,(1)} \quad (20)$$

It is noted that the SOC used in (21) for estimating capacity has to be a voltage-based $\text{SOC}_\text{V}$, which is inferred from OCV estimated in the first stage. The current-integration-based $\text{SOC}_\text{I}$ is not suitable for capacity estimation, because it requires the knowledge of capacity a priori to calculate $\text{SOC}_\text{I}$. It is worth mentioning that the combined SOC as a weighted average of $\text{SOC}_\text{v}$ and $\text{SOC}_\text{I}$ in [12] is also not suitable for capacity estimation, because the inclusion of $\text{SOC}_\text{I}$ forms a positive feedback loop and the capacity estimate is unable to recover from an incorrect initial capacity. However, the fluctuation in the OCV estimate may cause additional noise in the capacity estimate. Appropriate validity check and filtering schemes have to be designed accordingly to maintain the stability and robustness of the algorithm.

The two stage estimation consists of the following steps:

Step 1: Estimate OCV in real time from $V(k)$ and $I(k)$.

Step 2: Monitor the OCV validity signal for it becoming true for the first time. Save the $\text{SOC}_\text{V}$ as SOC(1) and start counting charge.

Step 3: Keep accumulating Charge as new current data come in. If the OCV validity signal is true, use the $\text{SOC}_\text{V}$ at that moment as SOC(k), and calculate the capacity $Q$ using (21). Set an output enabling flag true if there are enough updates. Continue Step 3 until the end of operation.

Step 4: If the output enabling flag is true, normalize $Q$ in terms of temperature.

The two algorithms for the driving mode are based on the same definition given in (6) and the same assumption that the relationship between OCV and SOC remains unchanged when a battery ages. The difference lies in that the one stage estimation algorithm accumulates $\Delta S$ only for one sampling time interval, while the two stage estimation algorithm

accumulates $\Delta S$ all the time since the OCV validity signal becomes true for the first time. Obviously the one stage estimation is more robust to the charge accumulation error caused by sensor imperfection. However, the tradeoff is that a local estimate of $h$ based on a small $\Delta S$ may have large fluctuation. Therefore, the two stage estimation is more stable in the sense that the capacity estimate stays in a smaller band during one entire driving cycle. In our design, the capacity estimates from both algorithms are combined via an adaptive weighting scheme for increased stability and robustness.

## IV. Estimation In The Plug-In Charge Mode

In the plug-in charge mode, the current is always in one direction and remains almost constant. Therefore the current can be considered as a DC current. Online recursive parameter estimation methods cannot be applied because there is no enough signal excitation for parameter convergence. Recall the two-RC-pair equivalent circuit model in (1). The dynamic voltages $V_{dl}(k)$ and $V_{df}(k)$ modeled by the RC pairs saturate after an initial time period in the plug-in charge mode. As the equivalent circuit model reaches steady state, the capacitors in the RC pairs can be considered an open circuit. Consequently the model described by (1) can be reduced into

$$V_{oc}(k) = V(k) - I(k)R \tag{21}$$

where $R$ denotes the sum of $R_{ohm}$ and the resistors in the RC pairs. The values of all the resistors can be estimated by a battery parameter estimation algorithm in the driving mode where there is enough signal excitation, such as the one presented in [12]. These values are stored in NVM, and will be read to calculate $R$ during the charge mode. It is noted that all the resistance values are temperature dependent and need to be normalized to a certain temperature before being stored into NVM. After reading the normalized resistance values from NVM, the capacity estimation algorithm also needs to reverse the normalization based on the present temperature to have a temperature dependent $R$. Since $R$ cannot be updated during plug-in charge, an assumption is needed, that is, $R$ will remain constant during plug-in charge. This assumption is satisfied within a certain range of SOC based on the experiments conducted on manganese-based Li-ion batteries. Such a range needs to be defined and calibrated for different batteries and plug-in charge strategies.

The capacity estimation algorithm in the plug-in charge mode consists of the following steps:

Step 1: In the plug-in charge mode, wait for a prescribed time period until double layer voltage and diffusion voltage saturate. Calculate normalized $R$ from the normalized resistance in NVM. Conduct inverse normalization to get $R$ at the present temperature.

Step 2: Read *V(k)* and *I(k)*. Calculate OCV based on (21). Find the corresponding SOC through a lookup table. If SOC is within a predefined range, go to Step 3. Otherwise repeat Step 2.

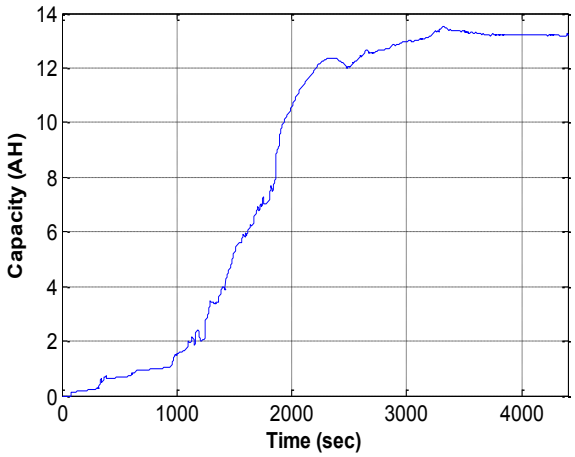


(a) Trajectory of capacity estimate from one stage estimation

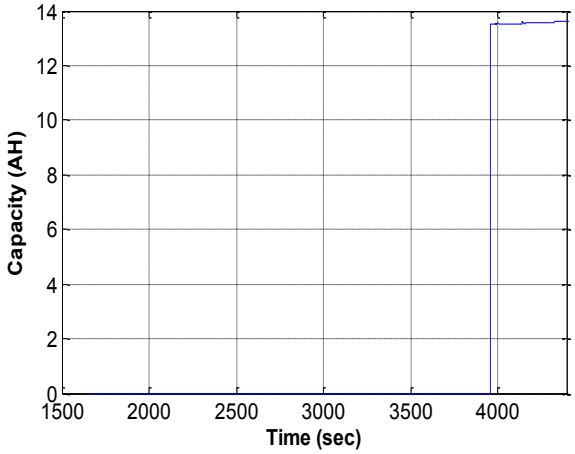


(b) Trajectory of capacity estimate from two stage estimation

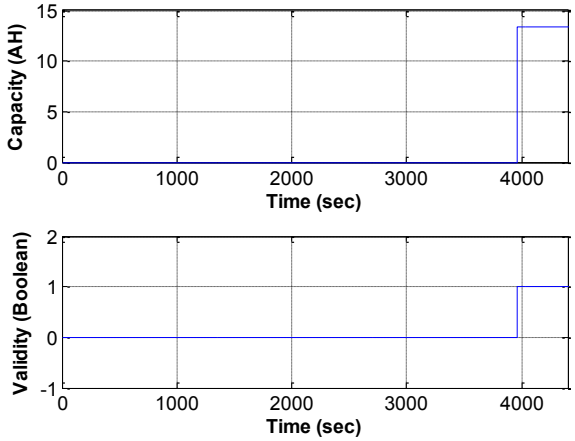


(c) Combined capacity estimate in the driving mode with its validity signal

Fig. 4. Algorithm evaluation for the driving mode with vehicle data.

Step 3: Start counting charge until OCV (i.e. SOC) reaches a specified threshold. Note that the threshold depends on the present temperature.

Step 4: Calculate battery capacity based on (20). Normalize the capacity to a defined temperature.

The algorithm is sensitive to current sensor accuracy. However, from many evaluation results, the algorithm shows

the ability to capture capacity fade very well and good robustness to the variation in $R$, as well as strong stability.

The estimated capacity is always blended with the past information stored in NVM. Different weights should be set for different algorithms for blending. The underlying principle is that the more frequently an algorithm gets a capacity update, the more its output should be weighted.

## V. RESULTS

The algorithms are evaluated with laboratory collected data and vehicle data. Fig. 4 shows the capacity estimation result from real vehicle driving data, for both algorithms for the driving mode. The measured capacity is 13.3AH, which is used as a reference value. Fig. 4(a) shows the convergence of the capacity estimate to the true capacity value for the one stage estimation. Fig. 4(b) shows the result from the two stage estimation. The algorithm starts to output a capacity estimate after 3,950 seconds when output enabling flag becomes true. The convergence speed is determined by the excitation level of SOC, which is dependent on the driving profile. Frequent updates of battery capacity are unnecessary as capacity changes slowly over the time. Fig. 4(c) shows a weighted combination of the two algorithms. The validity signal for the combined capacity estimate is also shown in Fig. 4(c).

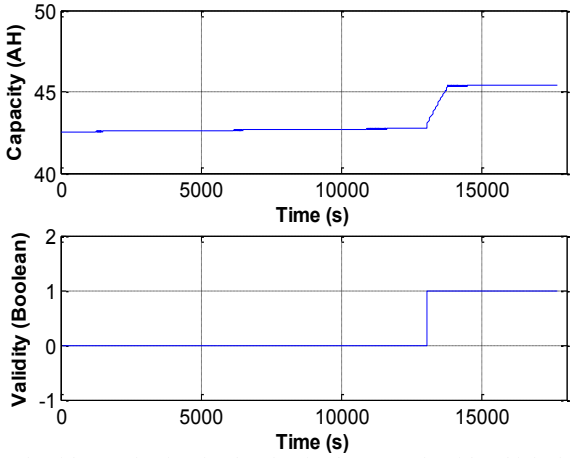


Fig.5. Algorithm evaluation for the plug-in charge mode with vehicle data.

Fig. 5 shows the evaluation result of the algorithm for the plug-in charge mode. The measured capacity of the pack is 45AH. The algorithm starts to output a capacity estimate after 13,000 seconds when OCV reaches a pre-defined threshold. Meanwhile the validity signal is set true as shown in Fig. 5.

Fig. 6 shows the evaluation results on accelerated aging data sets. In the accelerated aging test, the battery is cycled at high temperatures. Periodically the test is paused for checking capacity and collecting data excited by driving profiles. The data are fed to the algorithms and the estimated capacity is compared with the measured capacity for evaluation. Fig. 6 shows that the estimated capacity closely tracks the capacity fade as the battery ages.

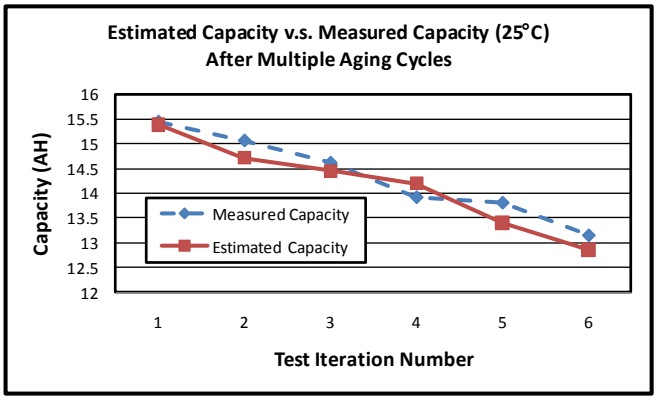


Fig. 6. Evaluation results with accelerated aging data.

## VI. CONCLUSION

In the paper, the capacity estimation for Li-ion batteries in PHEV/EV applications is studied. The focus is on the development of onboard algorithms for in-vehicle applications. Three algorithms are developed for the driving mode and the plug-in charge mode, respectively. The developed algorithms have been evaluated through laboratory collected data and vehicle data. The evaluation results demonstrate the close tracking of the measured capacity in terms of different ages of batteries.

## REFERENCES


[1] B. Y. Liaw, R. G. Jungst, G. Nagasubramanian, H. L. Case, and D. H. Doughty, "Modeling capacity fade in lithium-ion cells," *Journal of Power Sources*, vol. 140, pp. 157–161, 2005.

[2] B. S. Bhangu, P. Bentley, D. A. Stone, and C. M. Bingham, "Nonlinear observers for predicting state-of-charge and state-of-health of Lead-Acid batteries for hybrid-electric vehicles," *IEEE Transactions on Vehicular Technology*, vol. 54, pp. 783–794, 2005.

[3] A. T. Stamps, C. E. Holland, R. E. White, and E. P. Gatzke, "Analysis of capacity fade in lithium ion battery," *Journal of Power Sources*, vol. 150, pp. 229–239, 2005.

[4] P. Ramadass, B. Haran, R. White, and B. N. Popov, "Mathematical modeling of the capacity fade of Li-ion cells," *Journal of Power Sources*, vol. 123, pp. 230–240, 2003.

[5] G. Ning and B. N. Popov, "Cycle Life Modeling of Lithium-ion Batteries," *Journal of the Electrochemical Society*, vol. 151, issue 10, pp. 1584–1591, 2004.

[6] T. Kailath, A. H. Sayed, and B. Hassibi, *Linear Estimation*, Prentice Hall, 2000.

[7] V. Johnson, A. Pesaran, and T. Sack, "Temperature-dependent battery models for high-power lithium-ion batteries," in *Proceedings of the 17th Electric Vehicle Symposium*, Montreal, Canada, 15-18 Oct. 2000

[8] G. L. Plett, "Extended kalman filtering for battery management systems of LiPB-based HEV battery packs," *Journal of Power Sources*, vol. 134, pp. 252–292, 2004.

[9] S. J. Lee, J. H. Kim, J. M. Lee, and B. H. Cho, "The state and parameter estimation of an Li-ion battery using a new OCV-SOC concept", in 2007 *IEEE Power Electronics Specialists Conference*.

[10] G. J. Bierman, *Factorization Methods for Discrete Sequential Estimation*. New York: Academic, 1977.

[11] L. Ljung and T. Soderstrom, *Theory and Practice of Recursive Identification*. Cambridge, MA: MIT Press, 1983.

[12] X. Tang, X. Mao, J. Lin, and B. Koch, "Li-ion Battery Parameter Estimation for State of Charge", submitted to *2011 American Control Conference*.